

Design and inference for line transect surveys in occupancy studies

Milly Jones

School of Engineering, Mathematics and Physics, University of Kent, Canterbury, UK
email: mlj23@kent.ac.uk

and

Eleni Matechou

School of Mathematical Sciences, Queen Mary University of London, UK
email: e.matechou@qmul.ac.uk

and

Diana Cole

School of Engineering, Mathematics and Physics, University of Kent, Canterbury, UK
email: d.j.cole@kent.ac.uk

and

Robin Lines

Wildlife Conservation Society, Cambodia
email: rlines@wcs.org

and

Nicolas J. Deere

Durrell Institute of Conservation and Ecology (DICE), School of Natural Sciences,

University of Kent, Canterbury, UK

email: n.j.deere@kent.ac.uk

SUMMARY: Line transects, fixed paths along which observers record detections of animals or signs of their presence, are a core tool in ecological monitoring. Occupancy models commonly utilise line transect surveys to infer species' presence/absence in surveyed areas whilst accounting for imperfect detection and varying availability for detection along the transect. However, which ecological parameters can be inferred using such surveys depends on how detections are recorded, ranging from detection/non-detection in transect segments to continuous-time detections. We present the first comprehensive comparison of common line transect occupancy models within a unified framework, structured around data collection design, model formulation, parameter identifiability, and practical performance. We show that differing detection protocols give rise to structurally distinct statistical models, with varying identifiability properties and inferential performance. Using algebraic analysis and data cloning, we show that widely used models are often not practically identifiable. We develop a novel, data-based diagnostic to detect identifiability issues in applied settings and perform an extensive simulation study that illustrates the practical implications of data-collection approaches, model choice, and corresponding inference. We make recommendations regarding choice of detection protocol and line transect survey design and demonstrate the real-world consequences of these findings using a case study on leopards in the Zambesi-Transfrontier Conservation Area. Our results offer methodological innovation and actionable guidance for ecologists and statisticians.

KEY WORDS: Bayesian; Data cloning; Identifiability; Line transect studies; Occupancy models.

1. Introduction

Globally, biodiversity is declining at an unprecedented rate, reinforcing the need for wildlife monitoring methods that support reliable inference to guide conservation action (Gonzalez et al., 2023). Line transect surveys, fixed paths along which observers record detections of animals or signs of their presence, have become a cornerstone of such monitoring. Their appeal lies in logistical simplicity, scalability and ability to generate spatially structured data across large study regions (Hines et al., 2010; Whittington et al., 2015). They are routinely employed for large carnivore monitoring programmes (Hines et al., 2010; Lines et al., 2018; Sharma et al., 2024), for detecting signs of species poorly captured by emerging technologies (Wagner et al., 2025) and can be paired with new monitoring techniques such as telemetry and environmental DNA data (Kendall et al., 2023; Katayama et al., 2024) to validate ecological inference. Consequently, line transect data continue to be collected at scale and are increasingly used to inform high-stakes management decisions.

However, the spatial structure that makes transect surveys efficient also introduces statistical challenges. Line transect data are often analysed using occupancy models, a broad class of frameworks that infer species occupancy probabilities at surveyed sites whilst accounting for imperfect detection from detection/non-detection data (MacKenzie et al., 2002). Such models typically assume observations are independent, but detections collected along transects are rarely independent. Line transects often follow habitat features, such as rivers or roads, that are convenient for sampling whilst also functioning as low-resistance travel routes for wildlife. Consequently, detections recorded along transects are often spatially correlated. Ignoring this can result in bias and misleading inference (Hines et al., 2010), a pronounced problem when inference from transect surveys is expected to support management decisions and biased or unstable estimates can translate into misplaced conservation effort or delayed intervention.

The spatial autocorrelation in line transect data can be addressed using hierarchical

occupancy models that separate biological processes governing space use from the observation process that generates detections. During sampling, line transects are typically divided into segments of equal (and often arbitrary) length. Observers travel along the transects at a standardised pace and record, on each segment, direct encounters with animals or indirect signs of their presence such as dung or vocalizations (Hedges et al., 2013; Gestich et al., 2016); referred to as detections. A site is occupied if it intersects all or part of a species' home range during the sampling period. Within an occupied site, an individual transect segment is occupied if it intersects the home range. In this way, not all segments at occupied sites are used by the species, such as segments with high human footfall, which are routinely avoided by cryptic or sensitive species. An observer can only make detections on occupied segments (assuming no false positive observation error). Furthermore, detection probabilities on occupied segments are typically less than 1, so non-detection does not imply segment non-occupancy (false negative observation error). The detection process is therefore shaped by the spatial relationship between the species' home range, the sites and the transects, as illustrated schematically in Figure 1 a)i.

[Figure 1 about here.]

Building on this segment-level formulation, occupancy models for line transect data (also termed multi-scale single-season occupancy models, Nichols et al. (2008)) comprise three levels: site level occupancy, segment occupancy conditional on site occupancy, and detections conditional on segment occupancy. Spatial dependence in transect segments is most commonly modelled using discrete Markov processes (MP) (Hines et al., 2010; Whittington et al., 2015), with alternatives including intrinsic conditional autoregressive models (ICAR) (Crosby and Porter, 2018) and continuous-time Markov chain (CTMC) formulations (Guillera-Arroita et al., 2011). The segment-level detection data for these models depend critically on the detection protocol used, differing in their observation method and the num-

51 ber of observations made on each segment (segment-level replication). Common observation
52 methods include binary detection/non-detection protocols (DND - record a 1 if a detection
53 is made on a segment and a 0 otherwise) and counts (C - count of all detections on segment,
54 Emmet et al., 2021) which can be implemented without complex equipment. Distance to
55 first detection (DTD - distance between start of segment and first detection Henry et al.,
56 2020) observations are increasingly taken following technological improvements (for example
57 using camera time-stamps or GPS locations). Finally, independent replicate observations
58 per transect segment can be taken by multiple devices or observers (Nichols et al., 2008;
59 Whittington et al., 2015).

60 The choice of detection protocol is typically governed by cost, feasibility, and species
61 detectability. Critically, an overlooked criterion is their effect on model identifiability. While
62 the aforementioned occupancy models were introduced to account for spatial autocorrela-
63 tion in line transect data, they also introduce additional latent structure and associated
64 parameters. In the context of conservation monitoring, non-identifiability is particularly
65 problematic because parameters that cannot be uniquely identified from the data cannot
66 be estimated reliably, and non-identifiability can result in biased parameter estimates or
67 large variability (Cole, 2020). Identifiability issues can arise from inherent model structure
68 (structural non-identifiability) or from the underlying data set (practical non-identifiability).
69 In multi-scale occupancy models, confounding between occupancy and detection processes
70 has been identified previously and addressed through constraints or replicated observations
71 (Nichols et al., 2008; Kendall et al., 2013). Hines et al. (2010) reported convergence problems
72 in the absence of segment-level correlation, recommending aggregation of detection histories
73 and modelling segments as independent. These studies demonstrate that identifiability in line
74 transect occupancy models is highly sensitive to assumptions about spatial autocorrelation,
75 their explicit representation in the model, and the detection protocol used. Identifiability

76 issues caused by model formulation will cause inferential problems whether using frequentist
77 or Bayesian approaches. In the former these will often appear as convergence issues and in
78 Bayesian approaches will often result in poor mixing in chains. In this paper, we employ
79 Bayesian inference but employ uniform priors on all model probabilities so that results
80 regarding identifiability are applicable within a frequentist setting as well.

81 While recent work has explored how detection protocols affect site-level occupancy proba-
82 bilities (Pautrel et al., 2024), much less attention has been paid to segment-level occupancy
83 probabilities and their identifiability in the presence of spatial autocorrelation. Furthermore,
84 few guidelines exist for the effect of line transect design (such as length or number of
85 segments) despite the influence these have on parameter interpretations and resulting model
86 identifiability. This gap is particularly concerning given the potential of line transect surveys
87 to infer fine-scale space-use patterns. Increasingly, conservation questions extend beyond
88 simple presence or absence at the site level to understanding space use within home ranges,
89 such as episodic use of habitat elements to satisfy ecological demands (Wright and Hooten,
90 2025). Species' habitat preferences can be modelled as functions of environmental covariates
91 to quantify hierarchical habitat selection (McGarigal et al., 2016), providing information that
92 is critical for targeted management. Importantly, negative impacts on species often manifest
93 first at fine spatial resolutions through subtle changes in abundance or range contractions.
94 Such changes can serve as early warning indicators of population decline before site-level
95 extirpation becomes detectable through traditional occupancy analyses.

96 This paper places identifiability at the centre of line transect occupancy modelling. In
97 Section 2, we develop a unifying framework that classifies line transect occupancy mod-
98 els according to their latent segment occupancy process (L), detection protocol (O), and
99 number of independent replicate observations per segment (J), denoted L/O/J. In Section
100 3, we conduct an extensive simulation study to examine how these modelling and data-

101 collection choices affect identifiability and inference under ecologically realistic scenarios,
 102 with particular emphasis on spatial autocorrelation. Section 4 investigates identifiability
 103 and study-design considerations in detail and introduces a novel, data-based diagnostic for
 104 detecting identifiability problems using simple, cheap summaries of observed data, supported
 105 by extensive and computationally expensive data-cloning simulations. Finally, in Section 5,
 106 we apply our framework to leopard data from the Zambezi Trans-frontier Conservation Area,
 107 illustrating how detection protocol and transect design govern the reliability of fine-scale
 108 occupancy inference across the landscape and, ultimately, the value of line transect surveys
 109 for robust, timely conservation decision-making.

110 2. The Models

111 In this section, we develop the modelling framework introduced in Section 1. We consider
 112 S sites, where each site $i = 1, \dots, S$ is occupied independently with probability ψ . The
 113 occupancy status of site i , denoted $w_i \in \{0, 1\}$, follows $w_i \sim \text{Bern}(\psi)$. As is standard in
 114 occupancy models, site occupancy is assumed to remain unchanged over the sampling period
 115 (MacKenzie et al., 2002).

116 At site i , M_i transects of length L_{im} are surveyed, with total site effort $L_i = \sum_{m=1}^{M_i} L_{im}$.
 117 Each transect is divided into segments of constant length R , resulting in $K_{im} = L_{im}/R$
 118 segments for transect m at site i . Conditional on site occupancy, transect m may intersect
 119 wholly, partially, or not at all with the home range of the species (see Figure 1). A segment is
 120 occupied if it intersects with the species' home range. The latent segment occupancy status
 121 is denoted $z_{i,m,k} \in \{0, 1\}$ for segments $k = 1, \dots, K_{im}$ at site i and transect m .

122 This defines a general multi-scale occupancy model (Kery and Royle, 2015) comprising
 123 three linked processes: site-level occupancy, segment-level occupancy conditional on site

124 occupancy, and detections conditional on segment occupancy:

$$\begin{aligned}
 w_i &\sim \text{Bernoulli}(\psi) && \text{(site-level occupancy)} \\
 z_{i,m,k} \mid w_i &\sim \text{Bernoulli}(w_i \theta_{i,m,k}) && \text{(segment-level occupancy)} \\
 y_{i,m,k,j} \mid z_{i,m,k} &\sim f(z_{i,m,k}, \beta) && \text{(detection process)}
 \end{aligned}$$

125 where $\theta_{i,m,k}$ is the probability that segment k at site i and transect m is occupied (given
 126 site occupancy). We denote by $y_{i,m,k,j}$ the j -th replicate observation on that segment, where
 127 observations arise from a distribution with density function f and detection parameters β .
 128 Assuming no false positive detections can be made, when $z_{i,m,k} = 0$ the probability of making
 129 a detection under density function f across any replicate on that segment is zero.

130 As discussed in Section 1, it is common to model the segment occupancy process using
 131 a first order spatial MP. In this framework, if a segment is occupied, the next segment is
 132 occupied with probability θ_{11} , and if a segment is unoccupied, the next is occupied with
 133 probability θ_{01} . The first segment at occupied sites is occupied with probability η . It is
 134 common to assume stationarity with $\eta = \theta_{01}/[\theta_{01} + 1 - \theta_{11}]$ or to set $\eta = \theta_{01}$ (Hines et al.,
 135 2010); alternatively η can be estimated as an additional model parameter. Stationarity may
 136 be applicable if the transect begins in the middle of a trail, and $\eta = \theta_{01}$ may be applicable
 137 if the survey is started from a point where individuals are unlikely to occupy the preceding
 138 space (such as a forest boundary).

139 The models in this paper share the site occupancy and segment occupancy process de-
 140 scribed above but differ by the detection protocols, which we describe in Section 2.1. The
 141 different models are outlined in Figure 1 a), showing the latent segment occupancy, the
 142 observation methods, and replication in the observation process.

143 2.1 Detection process and model likelihoods

144 The general framework for likelihood functions for line transect occupancy models is:

$$\mathcal{L} = \prod_{i=1}^S \left\{ \psi \prod_{m=1}^{M_i} H_{i,m} + (1 - \psi) \mathbb{I}(\delta_i = 0) \right\}, \quad (1)$$

145 where δ_i is the number of species detections at site i and $H_{i,m}$ is the likelihood function
 146 for the observations at site i and transect m conditional on the site being occupied. The
 147 form of $H_{i,m}$ varies both by the segment occupancy model and the detection protocol. When
 148 modelling the latent segment occupancy process with a MP, $H_{i,m}$ takes the following form:

$$H_{i,m} = [1 - \eta, \eta] \left\{ \prod_{k=1}^{K_{im}-1} \text{diag}(P_{i,m,k}) \Theta \right\} P_{i,m,K_{im}},$$

149 where

$$\Theta = \begin{bmatrix} 1 - \theta_{01} & \theta_{01} \\ 1 - \theta_{11} & \theta_{11} \end{bmatrix},$$

150 and $P_{i,m,k} = [P_{i,m,k}^0, P_{i,m,k}^1]$. $P_{i,m,k}^0$ and $P_{i,m,k}^1$ are the probabilities of observations on segment
 151 k at site i and transect m conditional on $z_{i,m,k} = 0$ and $z_{i,m,k} = 1$ respectively.

152 In each of the following models, the latent segment occupancy process is modelled using a
 153 MP, and along occupied segments detections are modelled as a Poisson point process with
 154 rate λ . The probability of a single observer making at least one detection on an occupied
 155 segment of length R is $p = 1 - \exp(-\lambda R)$.

156 2.1.1 MP/DND/J. At site i , transect m , and segment k , $j = 1, \dots, J$ independent
 157 detection/non-detections observations, $h_{i,m,k,j} \in \{0, 1\}$, are made. Let $\delta_{i,m,k} = \sum_{j=1}^J h_{i,m,k,j}$
 158 denote the number of detections per segment k . Then:

$$P_{i,m,k} = [\mathbb{1}(\delta_{i,m,k} = 0), \prod_{j=1}^J p^{h_{i,m,k,j}} (1 - p)^{1-h_{i,m,k,j}}]^T$$

159 2.1.2 MP/DTD/J. At site i , transect m , and segment k , $j = 1, \dots, J$ independent
 160 measurements, $l_{i,m,k,j}$, are made between the start of the segment and the first detection. If

161 no detection is made, we let $l_{i,m,k,j} = R$. Then:

$$P_{i,m,k} = [\mathbb{1}(\delta_{i,m,k} = 0), \prod_{j=1}^J \lambda^{\mathbb{1}(l_{i,m,k,j} \neq R)} \exp(-\lambda l_{i,m,k,j})]^T$$

162 2.1.3 *MP/C/J*. At site i , transect m , and segment k , $j = 1, \dots, J$ independent counts
163 $c_{i,m,k,j}$ are made of the number of detections. Then:

$$P_{i,m,k} = [\mathbb{1}(\delta_{i,m,k} = 0), \prod_{j=1}^J \frac{(\lambda R)^{c_{i,m,k,j}} \exp(-\lambda R)}{c_{i,m,k,j}!}]^T$$

164 2.2 Assumptions

165 The modelling framework above makes the following assumptions, which are common to
166 occupancy models. The occupancy status of a site or segment is unchanged throughout
167 the survey period (otherwise known as closure). Relaxations to this assumption include
168 multi-season occupancy models (MacKenzie et al., 2003). Replicate detections on a segment
169 are independent given segment occupancy, and there are no false positives in the detection
170 process. Occupancy models can be relaxed to allow for false positives (Royle and Link, 2006).
171 In this paper we also assume that site occupancy probabilities, segment occupancy transition
172 probabilities, and detection probabilities are constant. However, the models readily extend
173 to parameters that vary as a function of site or segment level covariates, a point to which
174 we return in Section 6.

175 3. Simulations

176 In this section, we compare the mean square error (MSE) of posterior distributions of models
177 MP/DND/1, MP/DND/2, MP/DTD/1, MP/DTD/2, and MP/C/1 (see Web Appendix 1 for
178 a short description of each model) under a range of different parameter settings. In Section
179 1, the absence of correlation in segment occupancy in the MP/DND/1 model is identified as
180 a cause of convergence problems (Hines et al., 2010). We therefore simulate data varying the
181 amount of correlation in segment occupancy (as $\theta_{01} \rightarrow \theta_{11}$) under high and low detectability

182 p . We denote by β the true value and by $\hat{\beta}_q$ the q -th posterior sample of a parameter. For Q
 183 samples, we let the MSE for this parameter be $\frac{1}{Q} \sum_{q=1}^Q (\hat{\beta}_q - \beta)^2$. All models are implemented
 184 in NIMBLE (de Valpine et al., 2017) in R (R Core Team, 2025).

185 We simulate $n = 10$ sites, $M = 10$ transects, and $K = 20$ segments of length 500. All
 186 simulations fix $\psi = 0.75$. Data are simulated using the discrete latent MP process with
 187 $\theta_{11} = 0.7$ and $\theta_{01} \in \{0.2, 0.3, 0.4, 0.5, 0.6, 0.7\}$. The first segment on each transect is drawn
 188 from stationarity. We consider two levels of detectability, one high with $\lambda = 1/300$ ($p \approx 0.81$),
 189 and one low with $\lambda = 1/1200$ ($p \approx 0.34$). For each parameter set, we simulate $N = 100$ data
 190 sets where detections on occupied segments follow a Poisson process with rate λ ; detections
 191 are summarised according to the corresponding model. For example, detections per segment
 192 are binarised for MP/DND/1 or only the distance to first detection is kept for MP/DTD/1.
 193 Details on prior distributions and MCMC runs are in Web Appendix 2.

194 Figure 2 shows, for each model, boxplots of $\log(\text{MSE})$ for parameters ψ , p , θ_{01} and θ_{11} across
 195 $\theta_{01} \in \{0.2, 0.3, 0.4, 0.5, 0.6, 0.7\}$. The distribution of MSE for the site occupancy parameter,
 196 ψ , is comparable across values of θ_{01} and all models. However, MP/DND/1 generally has
 197 much higher MSE for parameters p , θ_{01} and θ_{11} compared to the other models. It is also
 198 the only model where MSE increases rapidly for all parameters as $\theta_{01} \rightarrow \theta_{11}$. Overall,
 199 Figure 2 indicates that MSE is reduced by using continuous observations (MP/DTD/1
 200 versus MP/DND/1) and by increasing replication at the segment level (MP/DTD/2 versus
 201 MP/DTD/1). Web Figure 1 shows results for $p \approx 0.34$; as expected, the MSE increases for
 202 parameters p , θ_{01} and θ_{11} for all models as detectability decreases. Results are comparable
 203 for ψ between low and high detectability. As in the high detectability case, MP/DTD/1
 204 continues to have on average the second highest MSE behind MP/DND/1 for parameters
 205 p , θ_{01} and θ_{11} .

206 Even under ideal conditions, when p is high, as $\theta_{01} \rightarrow \theta_{11}$ the MSE for MP/DND/1 increases

207 drastically across parameters p , θ_{01} , and θ_{11} . Since $\theta_{01} \rightarrow \theta_{11}$ corresponds to decreasing spatial
208 auto-correlation in segment occupancy, this leads to practical non-identifiability, which is
209 investigated in the next section.

210 [Figure 2 about here.]

211 4. Identifiability

212 This section explores the identifiability of the models described in Section 2, focusing on
213 the latent segment process and its implications for inference and survey design. Section 4.1
214 investigates structural identifiability using symbolic differentiation (Cole, 2020), and shows
215 identifiability issues occur when correlation in segment occupancy is zero. This leads to
216 practical non-identifiability when the correlation is close to zero. A method for diagnosing
217 this is data cloning (Ponciano et al., 2012). Data cloning assesses parameter identifiability
218 by replicating the observed data set, with the variances of practically identifiable parameters
219 scaling inversely to the number of data copies. This method is computationally very
220 demanding and requires expertise to fit. Section 4.2 introduces a novel data-based metric, Δ ,
221 as an indicator of correlation in the latent segment process. Crucially, we show that the data-
222 based metric, which is simple and computationally cheap, can diagnose when this problem
223 occurs. We explore the minimum number of segments required for identifiability using
224 symbolic differentiation (Section 4.3), and extend this through data cloning to reveal weak
225 identifiability at low segment numbers. Finally, in Section 4.4 we discuss the implications of
226 segment length for survey design.

227 4.1 Independence of spatial replicates

228 An identifiable model can have certain points in the parameter space that are non-
229 identifiable. These points can be identified algebraically using the methods outlined in
230 Cole (2020) and Web Appendix 3. We find that MP/DND/1 is non-identifiable when

$\theta_{01} = \theta_{11} = \theta$. At this point, whether a segment is occupied is independent of adjacent
 segments. As only a single replicate observation is taken ($J = 1$), this model reduces to
 the restricted three-level occupancy model Kery and Royle (2015). The observation process
 becomes $y_{i,m,k,1} | z_{i,m,k} \sim \text{Bernoulli}(z_{i,m,k} \times \theta \times p)$, and is known to be non-identifiable
 (Nichols et al., 2008) as it is only possible to estimate θp jointly. In other words, a
 known non-identifiable model is nested within the MP/DND/1 design. We find the other
 models remain identifiable when $\theta_{01} = \theta_{11} = \theta$. Although other points in the parameter
 space lead to non-identifiable models, these are linked with boundary conditions (at points
 $\psi = 0, p = \lambda = 0, \theta_{01} = 0, (\eta, \theta_{01}) = (0, 0)$, and $\theta_{11} = 1$ when $\eta = \theta_{01}/(\theta_{01} + 1 - \theta_{11})$), full
 details of which can be found in Web Appendix 3.

4.2 Metric Δ - the data diagnostic

Model identifiability issues occur for MP/DND/1 when $\theta_{01} = \theta_{11} = \theta$. This condition cannot
 be checked prior to analysis as the segment occupancy process is unobserved. However, the
 detection process is observed; in this section we consider the link between correlation in the
 latent segment occupancy process and the observed detection process.

Conditional on site occupancy, $\mathbb{P}(h_{i,m,k} = 1 | h_{i,m,k-1} = 1, w_i = 1)$ denotes the probability a
 detection is made on segment k given a detection was made on segment $k - 1$. Conversely,
 $\mathbb{P}(h_{i,m,k} = 1 | h_{i,m,k-1} = 0, w_i = 1)$ denotes the probability a detection is made on segment k
 given no detection was made on segment $k - 1$. We then have the following result.

THEOREM 1: *Let site i be occupied and the latent segment occupancy process be modelled
 as a MP. Let η be the stationary probability for segment occupancy, and $h_{i,m,k} \in \{0, 1\}$ denote
 detection or non-detection on segment k of transect m . Then the following holds:*

$$\mathbb{P}(h_{i,m,k} = 1 | h_{i,m,k-1} = 1, w_i = 1) = \theta_{11}p, \quad (2)$$

$$\mathbb{P}(h_{i,m,k} = 1 | h_{i,m,k-1} = 0, w_i = 1) = \frac{p\theta_{01}(1 - \theta_{11}p)}{1 - \theta_{11} + \theta_{01}(1 - p)}. \quad (3)$$

253 *Proof.* See Web Appendix 4.1

254 Equality between Equations (2) and (3) implies that $\theta_{01} = \theta_{11}$, $p = 0$, or $\theta_{11} = 1$. These are
 255 all points within the parameter space previously identified as leading to a non-identifiable
 256 model under MP/DND/1. The point $p = 0$ is a boundary point occurring when there are
 257 no detections. When η is modelled as the stationary probability and $\theta_{11} = 1$, then the first
 258 segment on all transects is occupied, and all subsequent segments must remain occupied,
 259 so that the MP is modelling a process in which no state switches occur. Finally, $\theta_{11} = \theta_{01}$
 260 means there is no correlation in the latent segment occupancy process.

261 We let $\Delta = \mathbb{P}(h_{i,m,k} = 1|h_{i,m,k-1} = 1, w_i = 1) - \mathbb{P}(h_{i,m,k} = 1|h_{i,m,k-1} = 0, w_i = 1)$ denote
 262 the magnitude of the difference in the conditional probabilities of observing a detection.
 263 This is a statistic that is easily calculated from observed detection/non-detection data,
 264 conditioning on site occupancy, and is a function of the detection probabilities p and segment
 265 occupancy parameters θ_{01}, θ_{11} . We have shown that $\Delta = 0$ leads to identifiability issues under
 266 MP/DND/1, and now further explore how Δ can indicate weakly-estimable parameters under
 267 different detection protocols.

268 Theoretical identifiability does not ensure practical identifiability, that is model parameters
 269 may be identifiable but weakly-estimable (Cole, 2020). We investigate this issue (across
 270 all models in the paper) as $\Delta \rightarrow 0$ using data cloning. Data cloning assesses parameter
 271 identifiability by replicating the observed data set D times and examining how parameter
 272 variances scale as the amount of data increases. If a parameter is practically identifiable,
 273 then its variance scales with $1/D$ (Ponciano et al., 2012). Fixing $\psi = 0.75$, $n = 10$ sites,
 274 $M = 10$ transects per site, and $K = 20$ segments per transect, 5 data sets are generated
 275 for each of 12 parameter settings (see Web Appendix 4.2 for full details). Each data set is
 276 cloned $D \in \{1, 2, 5, 10, 15, 20\}$ times (by copying the detection histories resulting in a data

277 set of nD sites). The scaled variances, $\sigma_D^2(\cdot)/\sigma_1^2(\cdot)$, are computed from posterior variances
 278 $\sigma_D^2(\cdot)$ for each parameter.

279 We compute the MSE of scaled variances with respect to expected scaled variances
 280 using $\sum_D \left(\frac{\sigma_D^2(\cdot)}{\sigma_1^2(\cdot)} - \frac{1}{D} \right)^2$ over $D \in \{1, 2, 5, 10, 15, 20\}$. Figure 3 shows $\log(\text{MSE})$ for scaled
 281 variances of each parameter and data set against Δ for each model. Ten data sets for
 282 MP/DND/1 were removed where $\Delta < 0.1$ as the chains did not converge due to identifiability
 283 problems. As Δ decreases, the MSE for MP/DND/1 increases - indicating that parameters
 284 become increasingly non-identifiable even when $\Delta > 0$. The MSE for MP/DND/1 is
 285 comparable to other models (across all parameters) when $\Delta \approx 0.5$. This corresponds to
 286 simulations with highly ideal model parameters: high detectability, and strong spatial auto-
 287 correlation in segment occupancy. The MSE for MP/DTD/1 increases at small values of
 288 Δ in all parameters, but is comparable to other models when $\Delta \geq 0.2$. This suggests that
 289 MP/DTD/1 is more robust to low detectability and lack of auto-correlation in detections
 290 than MP/DND/1, but less so than the other models considered. MP/C/1 shows increases in
 291 MSE for θ_{01} and θ_{11} when $\Delta \approx 0$. These five points correspond to simulation parameters with
 292 the lowest detectability rather than lack of spatial auto-correlation in segment occupancy.
 293 MP/DND/2 and MP/DTD/2 are stable across Δ , even when detectability is low, showing
 294 that increased segment-level replication improves inference.

295 Crucially, we show that MP/DND/1 requires not just the existence of, but strong
 296 correlation in segment occupancy and high detectability in order to be fully identifiable.
 297 Whilst data cloning can be used to investigate identifiability, this is difficult for non-experts
 298 and is time consuming. Figure The metric, Δ , offers a practical and easy to use alternative
 299 that picks up when there is an issue of practical identifiability. Future data sets under this
 300 modelling framework can be quickly assessed for identifiability concerns using Δ , and it can
 301 serve as a tool to guide study design (more in Section 4.4).

[Figure 3 about here.]

4.3 Study Design

We investigate, under a range of different modelling assumptions, the number of segments required per transect to fully identify model parameters using symbolic differentiation (Cole, 2020) (full details in Web Appendix 5.1). We consider $K_{im} = 2, 3$, and 4 segments per transect, where 2 segments is the minimum to justify a MP to model segment occupancy. We look at whether ψ is to be estimated or assumed known and equal to 1 (for example where occupancy is known from other data in integrated models), and common forms for η . Results are shown in Web Tables 4 - 8 (in Web Appendix 5.1); table entries denote the deficiency in model identifiability, with 0 showing that the model is identifiable, or the level of deficiency otherwise. Web Table 4, for MP/DND/1, shows that $K = 4$ segments are required to guarantee model identifiability for all modelling constraints considered. Although fewer segments could be used, this would prevent analysis of the data under different constraints if required. Results for other models show that $K = 3$ segments are required across constraints in the same way. Practitioners should ensure that these conditions are met independently of the Δ value for the data set.

Since theoretical identifiability does not ensure practical estimability, we use data cloning to assess how estimability varies with the number of segments K . We take $n = 10$ sites, $M = 10$ transects per site, and vary $K \in \{4, 6, 8, 10, 15, 20\}$. We fix $\psi = 0.75$, $\theta_{11} = 0.7$, and $\theta_{01} = 0.1$ and let the first segment on each transect be drawn from stationarity. The detection rate is $\lambda = 1/300$ ($p \approx 0.81$). These parameter values have $\mathbb{E}(\Delta) = 0.46$ which is sufficiently great to distinguish the effects of K from the effect of spatial auto-correlation in segment occupancy. We generate $N = 10$ data sets for each K , and clone the data $D \in \{1, 2, 5, 10, 15, 20\}$ times. For full details see Web Appendix 5.2.

Figure 4 shows the box plot of $\log(\text{MSE})$ of scaled variances across K for parameters p ,

327 θ_{01} , and θ_{11} and each of the models. For MP/DND/1, the MSE increases as the number of
 328 segments decreases, and is greater than for other models when K is small. Whilst $K = 4$
 329 ensures identifiability, model parameters for MP/DND/1 are weakly estimable and require
 330 far more segments to be strongly estimable. Results for models MP/DND/2, MP/DTD/1,
 331 MP/DTD/2, and MP/C/1 show that the distribution of MSE is relatively constant across
 332 K , and so model parameters remain estimable even at low number of segments.

333 [Figure 4 about here.]

334 4.4 Choosing segment lengths

335 The segment length R and number of segments K per transect are closely related in survey
 336 design. In this section, we show that the choice of R has a considerable impact on Δ , and
 337 thus may determine the identifiability of the resulting survey data. The true latent process
 338 is likely to be continuous and we consider modelling occupancy along the transect using a
 339 continuous time Markov chain (CTMC). Whilst the transect is occupied, detections are again
 340 made according to a Poisson process with rate λ . This formulation describes an interrupted
 341 Poisson process (IPP), full details of which are in Web Appendix 6.1. Under this modelling
 342 framework, we find $\mathbb{P}(h_{i,m,k} = 1|h_{i,m,k-1} = 1, w_i = 1)$ and $\mathbb{P}(h_{i,m,k} = 1|h_{i,m,k-1} = 0, w_i = 1)$,
 343 and derive the following result:

344 **THEOREM 2:** *Let the site be occupied, the latent segment occupancy process be modelled*
 345 *using a CTMC, η be the stationary probability of occupancy at the start of the transect, and*
 346 *$h_{i,m,k} \in \{0, 1\}$ denote detection or non-detection on segment k of transect m . Let segments*
 347 *have length R . Then the following holds:*

$$\lim_{R \rightarrow \infty} \Delta = \lim_{R \rightarrow \infty} \left\{ \mathbb{P}(h_{i,m,k} = 1|h_{i,m,k-1} = 1, w_i = 1) - \mathbb{P}(h_{i,m,k} = 1|h_{i,m,k-1} = 0, w_i = 1) \right\} = 0. \quad (4)$$

348 *Proof.* See Web Appendix 6

Equation (4) confirms the known pattern that longer segments reduce correlations in detections—consistent with Hines et al. (2010), who recommend aggregating detection histories to weaken spatial dependence and enable independent segment modelling. Web Figure 2 shows how Δ varies with segment length R (for fixed transect length) across simulated detection rates (low-high) and switching rates between occupied and unoccupied states (low-high). As R increases, the mean Δ approaches zero in all scenarios, while variability rises because fewer segments, K , are observed. Across simulations, there is a segment length R that maximises the expected Δ , though under low detection and high switching rates, Δ remains flat. The maximal Δ also varies considerably between simulations. The maximal Δ increases with detection rate and lower switching (i.e. larger home ranges). Therefore, there may exist no R that guarantees sufficient identifiability for a chosen detection protocol. Theorem 2 and Web Figure 2 show that segment length as well as species characteristics (such as home range sizes and detectability) substantially impact Δ . Selecting an appropriate R thus determines which detection protocols are expected to lead to identifiable models in practice.

5. Case Study

We consider a case study of apex predators in the Kavango-Zambezi Transfrontier Conservation Area (KAZA TFCA) focussing here on the leopard (*Panthera pardus*) (Lines et al., 2018). From May to October 2015, a systematic randomized spoor and sightings survey was conducted on foot over 102 4-km transects mapped onto road networks (Lines et al., 2018). Each transect was visited $J = 3$ times over 10 days, and detection/non-detection data recorded on each segment of length 1km ($K = 4$). The surveyed region comprised $n = 10$ sites, with between $M = 8$ and 19 transects per site (see Figure 6 (a) for the distribution of transects over the KAZA TFCA). There were a total of 279 leopard sign detections over the 1224 segments, made at 61 of the 102 transects and 7 of the 10 sites.

The data are analysed using MP/DND/1, MP/DND/2, and MP/DND/3, and we assume

374 that the segment occupancy process starts at stationarity. See Web Appendix 7 for details
 375 on prior distributions and for posterior convergence summaries for each parameter. For
 376 $J = 1$ we have $\Delta = 0.303$, $J = 2$ gives $\Delta = 0.382$, and $J = 3$ gives $\Delta = 0.382$.
 377 Figure 3 indicates that for this value of Δ , MP/DND/1 is likely to experience identifiability
 378 problems for parameters p and θ_{11} . Furthermore, Figure 4 shows that identifiability issues
 379 are likely for these parameters when $K = 4$ segments are used. Figure 5(a) shows posterior
 380 means (circles) and 95% posterior credible intervals (PCIs -bars) for each model and model
 381 parameter. MP/DND/2 and MP/DND/3 show narrower PCIs in model parameters p and
 382 θ_{11} than MP/DND/1. Posterior distributions are comparable for ψ . Figure 5(b) shows the
 383 scaled variances for $D \in \{1, 2, 3, 4, 5, 10, 15, 20\}$ data clones. For each model parameter,
 384 MP/DND/2 and MP/DND/3 show a scaled variance that decreases in line with $1/D$.
 385 However, MP/DND/1 shows slower decrease for p and θ_{11} , and faster for θ_{01} . These results
 386 are consistent with those from Section 4.

387 Posterior means for θ_{11} for MP/DND/2 and MP/DND/3 are high, indicating a high
 388 probability that a segment following an occupied one is also occupied. This suggests the
 389 species uses the road network to facilitate long distance travel. Conversely, results for θ_{01}
 390 indicate a low probability of the species occupying the next segment if the current one
 391 is unoccupied. This inference is supported by Figure 6(a), which shows the placement of
 392 the transects within each of the 10 named sites, and Figures 6 (b), (c), and (d) which
 393 show the posterior probabilities of segment occupancy for models MP/DND/1, MP/DND/2,
 394 and MP/DND/3 respectively. Figure 6 shows that leopards widely use transect segments in
 395 the north-eastern region of the study area, and are largely absent from the south-western
 396 region. Crucially, this fine-scale map of leopards' use of the transects show that site level
 397 occupancy probabilities would miss details such as the spatial heterogeneity of segment
 398 occupancy at sites 'Moo' and 'Kalo'. Both these sites lie on the boundary between occupied

399 and non-occupied sites, highlighting how spatial use of the site becomes more fragmentary
400 towards boundaries of the species' home range. Finally, we can see that posterior probabilities
401 for model MP/DND/1 are more often close to 0.5 than they are for MP/DND/2 and
402 MP/DND/3. This indicates greater uncertainty about latent segment occupancy states when
403 only $J = 1$ replicate is used. This follows naturally from Figure 5(a), where the PCIs for
404 θ_{11} were much wider when $J = 1$ than when $J = 2$ or $J = 3$. Issues with model parameter
405 estimability therefore lead to considerably poorer inference about segment occupancy and
406 hinder the ability to create reliable fine-scale maps of occupancy.

407 [Figure 5 about here.]

408 [Figure 6 about here.]

409 6. Discussion

410 Occupancy models are widely used in species monitoring programmes. In multi-scale
411 designs where spatial autocorrelation among segments must be accounted for, Markov
412 process models for segment occupancy are commonly applied. Using algebraic results and
413 extensive simulation, this paper demonstrates that, despite being widely used, the single-
414 replicate detection/non-detection per segment model with a Markovian latent process is
415 particularly susceptible to identifiability issues. In contrast, continuous detection protocols
416 (such as distance-to-first-detection and count data) and replicated segment-level designs
417 are considerably more robust. We present a unified framework for analysing line transect
418 data within occupancy models, enabling direct comparison of inferential performance across
419 detection protocols. Simulation results show that the data-based diagnostic, Δ , derived from
420 detection correlations, effectively identifies identifiability issues, with both segment number
421 and length strongly influencing parameter identifiability. Together, these results provide
422 practical guidance for designing more reliable surveys.

423 We make the following recommendations for survey design. Single detection/non-detection
424 observations per segment are the most susceptible to identifiability problems. Continuous
425 detection protocols, such as distance-to-first-detection or count data, generally produce lower
426 bias, reduced uncertainty, and fewer identifiability issues, consistent with previous findings
427 (Henry et al., 2020). However, gains from distance-to-first-detection protocols are limited
428 under low detectability, and identifiability issues persist when data are sparse. Increasing
429 segment-level observations substantially improves robustness, reducing sensitivity to low
430 detectability and weak spatial dependence. In some cases replicated detection/non-detection
431 designs outperform continuous protocols. Careful attention must be paid to the closure
432 assumption when increasing replication; further investigation into fractional replication
433 (where only a subset of sites are revisited; Doser and Stoudt, 2023) may show improved
434 robustness while remaining feasible. Accordingly, when data are collected continuously, we
435 strongly recommend against aggregating them into single-replicate detection/non-detection
436 observations; aggregating to segment counts offers greater robustness than distance-to-
437 first-detection. Overall, replicated segment-level observations are most robust, with both
438 detection/non-detection and distance-to-first-detection performing comparably.

439 Choice of segment length and number is a critical but often overlooked element of survey
440 design. While four segments per transect are theoretically sufficient for identifiability in
441 single-replicate detection/non-detection models, substantially more are needed for reliable
442 estimation. Similarly, four segments per transect are generally sufficient for continuous
443 detection protocols and replicated segment-level observations when detectability is high.
444 Practically, the primary consideration should be segment length rather than segment number,
445 though these are closely linked. Segment length influences spatial dependence in detections
446 across segments and, in turn, identifiability under single-replicate detection/non-detection
447 and distance-to-first-detection protocols. As line transect surveys typically collect data con-

448 tinuously, we propose a post-hoc optimisation to guide model selection and data processing.
449 Segment lengths should vary from near zero to one-quarter of the transect length, discretising
450 the data at each step. The optimal segment length maximises the metric Δ . If $\Delta < 0.5$ at the
451 optimum, we recommend against single-replicate detection/non-detection models; if $\Delta < 0.2$,
452 we recommend against single-replicate distance-to-first-detection models. When continuous
453 data collection is infeasible at large scale, a pilot study can optimise segment length and
454 detection protocol for future surveys by recording detection locations and applying the same
455 optimisation method. These recommendations extend to legacy line transect data, allowing
456 re-analysis with more robust models that reduce bias and uncertainty. For historic data
457 sets restricted to single-replicate detection/non-detection observations, the diagnostic Δ can
458 assess the reliability and identifiability of parameter estimates.

459 Across all simulation scenarios, estimates of site-level occupancy ψ were relatively robust,
460 consistent with previous findings (Pautrel et al., 2024), and comparable across detection
461 protocols. However, when the inferential focus shifts to detection or segment-level occupancy,
462 parameters critical for understanding fine-scale space use and hierarchical habitat selection,
463 survey design choices become more influential. This was particularly evident in the leopard
464 case study in the KAZA-TFCA, where segment-level occupancy revealed detailed spatial
465 variation toward home range edges, patterns missed at the site level. The single-replicate
466 detection/non-detection protocol, however, showed substantially greater uncertainty than
467 multi-replicate designs.

468 We excluded covariates to establish the baseline identifiability of each model, following
469 recommendations that covariates should not be used to resolve non-identifiability (Kery and
470 Royle, 2015). Extending the framework to incorporate heterogeneous observation protocols
471 (for example, mixing discrete and continuous detections) and sign types (spoor vs. scat) is fea-
472 sible, if independence assumptions are maintained, to alleviate time and resource constraints

473 in field surveys. While our recommendations focus on single-species frameworks, further
474 work should extend these results to multi-species and multi-season models, particularly
475 where species behaviour or detectability differences influence design. Although we focus on
476 Markov process latent dynamics and often assume stationarity, alternative latent processes
477 and non-stationary initial conditions warrant investigation, especially on short transects,
478 where misspecification may bias inference (Crosby and Porter, 2018).

479 This study provides the first comprehensive exploration of identifiability under multi-scale
480 occupancy models with Markovian latent processes. By linking identifiability to directly
481 observable data, we present an accessible approach to diagnosing and optimising survey
482 design. While specific recommendations depend on species traits such as detectability and
483 home-range size, our results establish a mechanism by which an optimal model can be
484 selected. Broadly, species with low detectability and small home ranges require continuous
485 detection protocols or segment-level replication to ensure robust inference. More generally,
486 this optimisation-based approach provides a transparent, data-driven foundation for design-
487 ing and evaluating species monitoring programmes, allowing practitioners to tailor strategies
488 that maximise identifiability and minimise uncertainty in ecological inference.

489

FUNDING

490 The PhD project of the corresponding author, MJ, is funded by the Engineering and Physical
491 Sciences Research Council. NJD was supported by a Leverhulme Trust Research Leader
492 Award to Dr Matthew J. Struebig.

493

SUPPLEMENTARY MATERIALS

494 Supplementary material is available at Biometrics online. Web Appendices, Tables, and
495 Figures referenced in Sections 4-5 are available with this paper at the Biometrics website on
496 Oxford Academic.

497

DATA AVAILABILITY

498 The R code and case study data used in this paper to support our findings are available at
499 <https://github.com/millyljones/Line-Transect-Occupancy>

500

REFERENCES

- 501 Cole, D. J. (2020). *Parameter Redundancy and Identifiability*. CRC Press.
- 502 Crosby, A. D. and Porter, W. F. (2018). A spatially explicit, multi-scale occupancy model for
503 large-scale population monitoring. *The Journal of Wildlife Management* **82**, 1300–1310.
- 504 de Valpine, P., Turek, D., Paciorek, C., Anderson-Bergman, C., Temple Lang, D., and Bodik,
505 R. (2017). Programming with models: writing statistical algorithms for general model
506 structures with NIMBLE. *Journal of Computational and Graphical Statistics* **26**, 403–
507 413.
- 508 Doser, J. W. and Stoudt, S. (2023). “Fractional replication” in single-visit multi-season
509 occupancy models: Impacts of spatiotemporal autocorrelation on identifiability. *Methods*
510 *in Ecology and Evolution* .
- 511 Emmet, R. L., Long, R. A., and Gardner, B. (2021). Modeling multi-scale occupancy for
512 monitoring rare and highly mobile species. *Ecosphere* **12**,.
- 513 Gestich, C. C., Caselli, C. B., Nagy-Reis, M. B., Setz, E. Z., and da Cunha, R. G. (2016).
514 Estimating primate population densities: the systematic use of playbacks along transects
515 in population surveys. *American Journal of Primatology* **79**, e22586.
- 516 Gonzalez, A., Vihervaara, P., Balvanera, P., Bates, A. E., Bayraktarov, E., Bellingham, P. J.,
517 Bruder, A., Campbell, J., Catchen, M. D., Cavender-Bares, J., et al. (2023). A global
518 biodiversity observing system to unite monitoring and guide action. *Nature Ecology &*
519 *Evolution* **7**, 1947–1952.
- 520 Guillera-Aroita, G., Morgan, B. J. T., Ridout, M. S., and Linkie, M. (2011). Species

- 521 occupancy modeling for detection data collected along a transect. *Journal of Agricultural,*
522 *Biological, and Environmental Statistics* **16**, 301–317.
- 523 Hedges, S., Johnson, A., Ahlering, M., Tyson, M., and Eggert, L. S. (2013). Accuracy,
524 precision, and cost-effectiveness of conventional dung density and fecal DNA based survey
525 methods to estimate Asian elephant (*Elephas maximus*) population size and structure.
526 *Biological Conservation* **159**, 101–108.
- 527 Henry, D. A. W., Lee, A. T. K., and Altwegg, R. (2020). Can time-to-detection models
528 with fewer survey replicates provide a robust alternative to traditional site-occupancy
529 models? *Methods in Ecology and Evolution* **11**, 643–655.
- 530 Hines, J. E., Nichols, J. D., Royle, J. A., MacKenzie, D. I., Gopalaswamy, A. M., Kumar,
531 N. S., and Karanth, K. U. (2010). Tigers on trails: occupancy modeling for cluster
532 sampling. *Ecological Applications* **20**, 1456–1466.
- 533 Katayama, N., Yamamoto, S., Baba, Y. G., Ito, K., and Yamasako, J. (2024). Complementary
534 role of environmental DNA for line-transect bird surveys: A field test in a Japanese rice
535 landscape. *Ecological Indicators* **166**, 112442.
- 536 Kendall, C. J., Bracebridge, C., Lynch, E. C., Mgumba, M., Monadjem, A., Nicholas, A., and
537 Kane, A. (2023). Value of combining transect counts and telemetry data to determine
538 short-term population trends in a globally threatened species. *Conservation Biology* **37**,
- 539 Kendall, W. L., Hines, J. E., Nichols, J. D., and Grant, E. H. C. (2013). Relaxing the closure
540 assumption in occupancy models: staggered arrival and departure times. *Ecology* **94**,
541 610–617.
- 542 Kery, M. and Royle, J. A. (2015). *Applied Hierarchical Modeling in Ecology Analysis of*
543 *Distribution, Abundance and Species Richness in R and Bugs - Prelude and Static*
544 *Models*. Elsevier Science & Technology Books.
- 545 Lines, R., Tzanopoulos, J., and MacMillan, D. (2018). Status of terrestrial mammals at

- 546 the Kafue–Zambezi interface: implications for transboundary connectivity. *Oryx* **53**,
547 764–773.
- 548 MacKenzie, D. I., Nichols, J. D., Hines, J. E., Knutson, M. G., and Franklin, A. B. (2003).
549 Estimating site occupancy, colonization, and local extinction when a species is detected
550 imperfectly. *Ecology* **84**, 2200–2207.
- 551 MacKenzie, D. I., Nichols, J. D., Lachman, G. B., Droege, S., Royle, J., and Lagtim, C. A.
552 (2002). Estimating site occupancy rates when detection probabilities are less than one.
553 *Ecology* **83**, 2069–2360.
- 554 McGarigal, K., Wan, H. Y., Zeller, K. A., Timm, B. C., and Cushman, S. A. (2016). Multi-
555 scale habitat selection modeling: a review and outlook. *Landscape Ecology* **31**, 1161–1175.
- 556 Nichols, J. D., Bailey, L. L., O’Connell Jr., A. F., Talancy, N. W., Campbell Grant, E. H.,
557 Gilbert, A. T., Annand, E. M., Husband, T. P., and Hines, J. E. (2008). Multi-scale
558 occupancy estimation and modelling using multiple detection methods. *Journal of*
559 *Applied Ecology* **45**, 1321–1329.
- 560 Pautrel, L., Moulherat, S., Gimenez, O., and Etienne, M. (2024). Analysing biodiversity
561 observation data collected in continuous time: Should we use discrete- or continuous-
562 time occupancy models? *Methods in Ecology and Evolution* .
- 563 Ponciano, J. M., Burleigh, J. G., Braun, E. L., and Taper, M. L. (2012). Assessing Parameter
564 Identifiability in Phylogenetic Models Using Data Cloning. *Systematic Biology* **61**,
565 955–972.
- 566 R Core Team (2025). *R: A Language and Environment for Statistical Computing*. R
567 Foundation for Statistical Computing, Vienna, Austria.
- 568 Royle, J. A. and Link, W. A. (2006). Generalized site occupancy models allowing for false
569 positive and false negative errors. *Ecology* **87**, 835–841.
- 570 Sharma, K., Alexander, J. S., Durbach, I., Kodi, A. R., Mishra, C., Nichols, J., MacKenzie,

- 571 D., Ale, S., Lovari, S., Modaqiq, A. W., Zhi, L., Sutherland, C., Khan, A. A., McCarthy,
572 T., and Borchers, D. (2024). Chapter 34 - PAWS: Population Assessment of the World's
573 Snow leopards. In Mallon, D. and McCarthy, T., editors, *Snow Leopards (Second*
574 *Edition)*, Biodiversity of World: Conservation from Genes to Landscapes, pages 437–
575 447. Academic Press, Second edition.
- 576 Wagner, B., Garnick, S. W., Ryan, M. F., Isaac, J. L., Begg, A., and Nitschke, C. R. (2025).
577 Thermal drone surveys to detect arboreal fauna: Improving population estimates and
578 threatened species monitoring. *Ecological Applications* **35**,
- 579 Whittington, J., Heuer, K., Hunt, B., Hebblewhite, M., and Lukacs, P. M. (2015). Estimating
580 occupancy using spatially and temporally replicated snow surveys. *Animal Conservation*
581 **18**, 92–101.
- 582 Wright, W. J. and Hooten, M. B. (2025). Continuous-space occupancy models. *Biometrics*
583 **81**,

Received October 2007. Revised February 2008. Accepted March 2008.

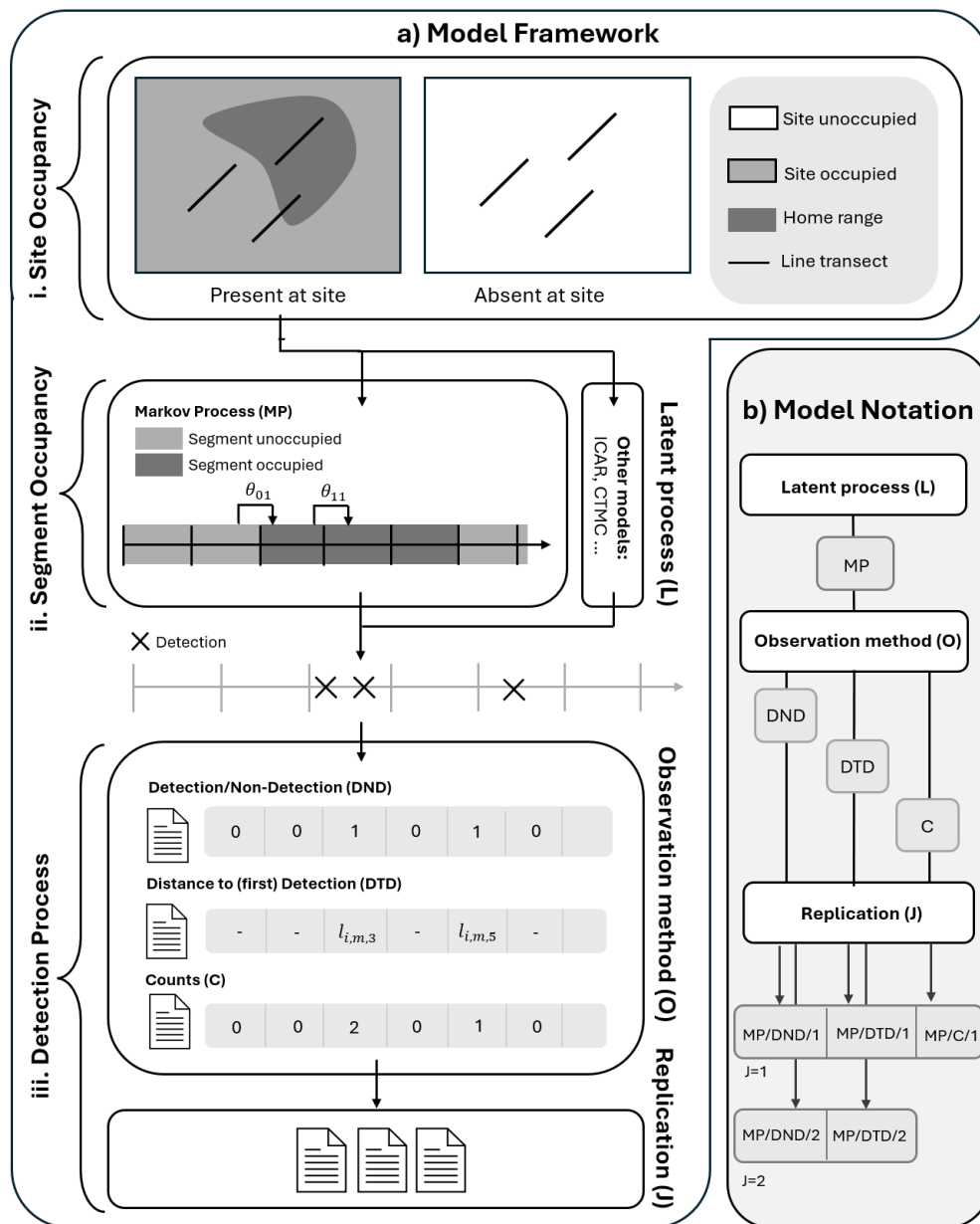


Figure 1. a) Modelling framework including site occupancy, segment occupancy and the detection process. i. A site may be unoccupied or occupied, with transects wholly, partially, or not intersecting the home range of species' at occupied sites. ii. The latent segment occupancy process models the intersection of transects with the home range. iii. The detection process comprises the observation method and replication of observations. b) Models are labelled L/O/J according to their latent segment occupancy process (L), observation method (O), and amount of replication (J)

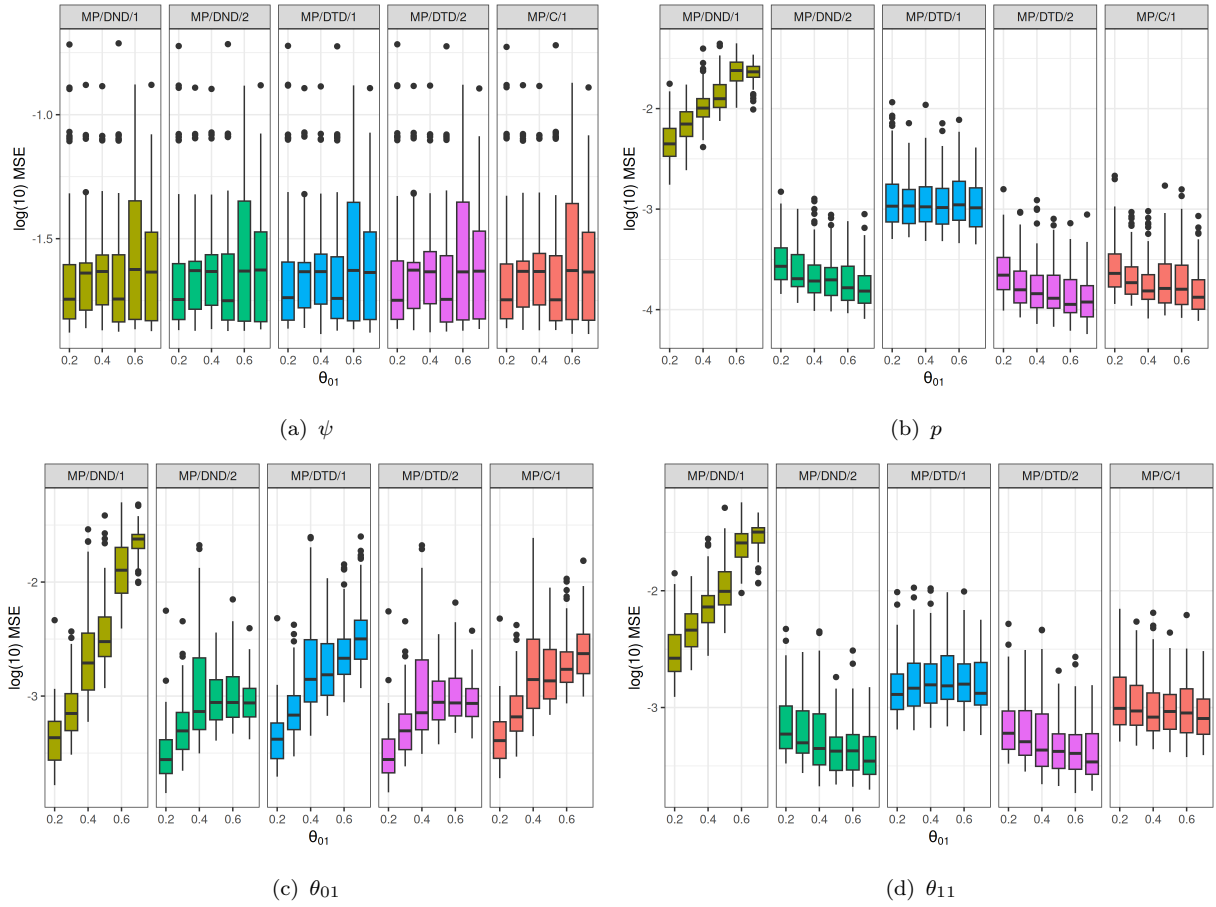


Figure 2. Boxplot of $\log(\text{MSE})$ for parameters ψ , p , θ_{01} and θ_{11} across $\theta_{01} \in \{0.2, 0.3, 0.4, 0.5, 0.6, 0.7\}$ when $\theta_{11} = 0.7$ and $p \approx 0.81$, for models MP/DND/1, MP/DND/2, MP/DTD/1, MP/DTD/2, MP/C/1.

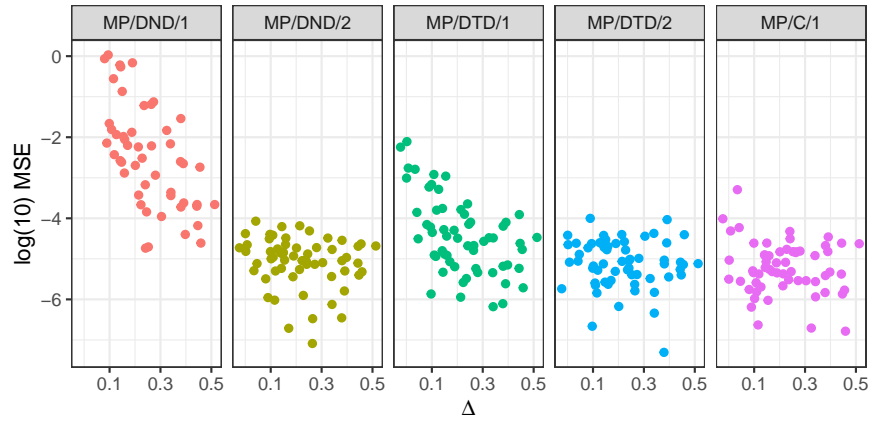
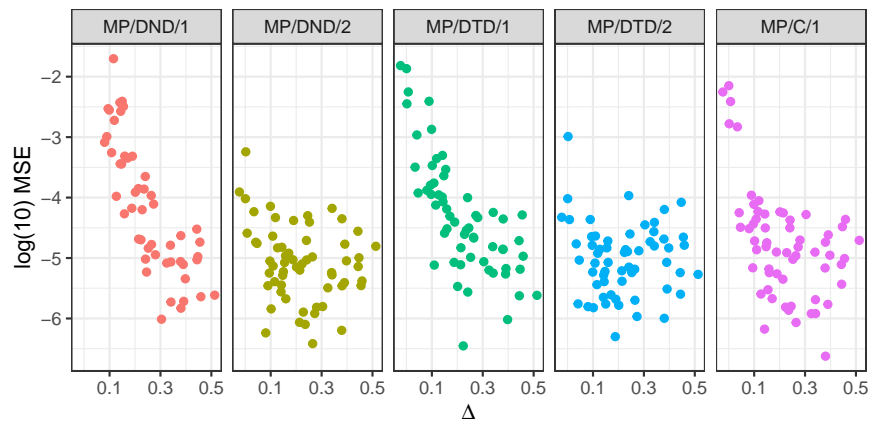
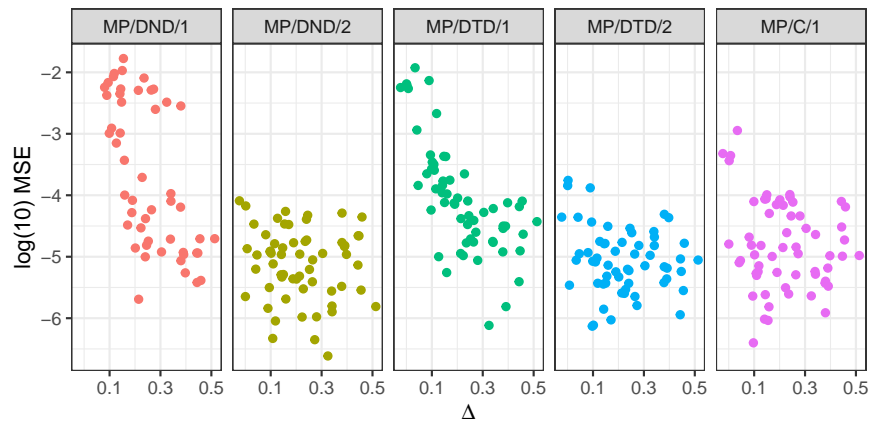
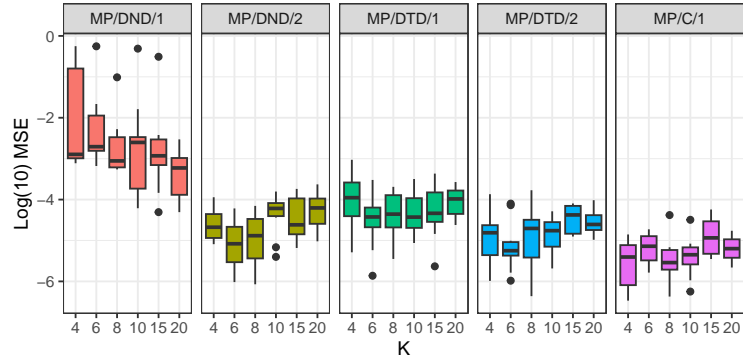
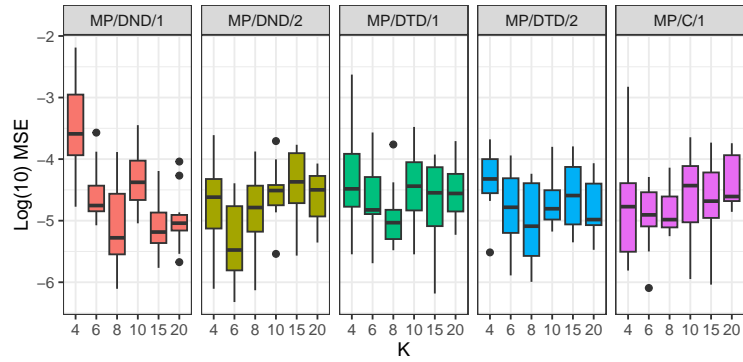
(a) p (b) θ_{01} (c) θ_{11}

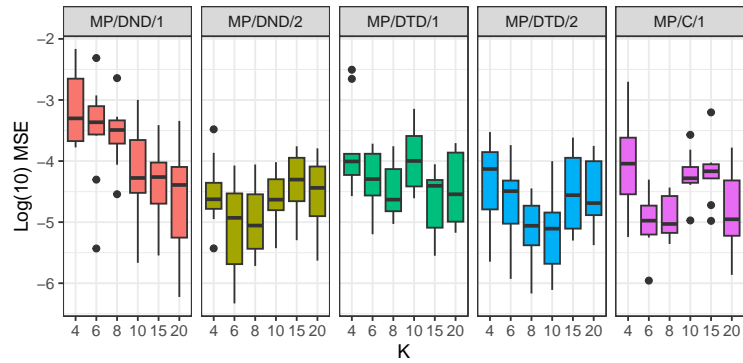
Figure 3. Log(10) MSE for parameters p , θ_{01} and θ_{11} across metric values Δ and models MP/DND/1, MP/DND/2, MP/DTD/1, MP/DTD/2, MP/C/1.



(a) p



(b) θ_{01}



(c) θ_{11}

Figure 4. Log(10) MSE for parameters p , θ_{01} and θ_{11} across number of segments $K \in \{4, 6, 8, 10, 15, 20\}$ and models MP/DND/1, MP/DND/2, MP/DTD/1, MP/DTD/2, MP/C/1.

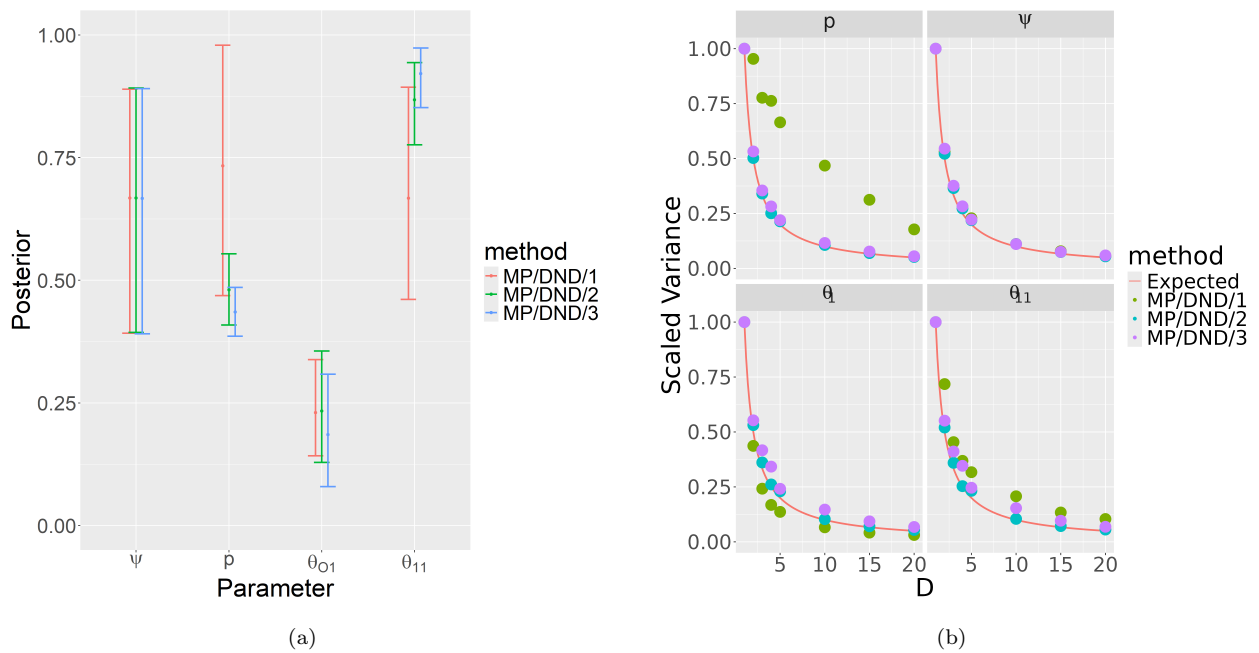


Figure 5. (a) Posterior means (circles) and 95% PCIs (bars) for MP/DND/1, MP/DND/2, and MP/DND/3. (b) Scaled variances (points) for models MP/DND/1, MP/DND/2, and MP/DND/3 for $D \in \{1, 2, 3, 4, 5, 10, 15, 20\}$. The expected scaled variance $1/D$ is the plotted line.

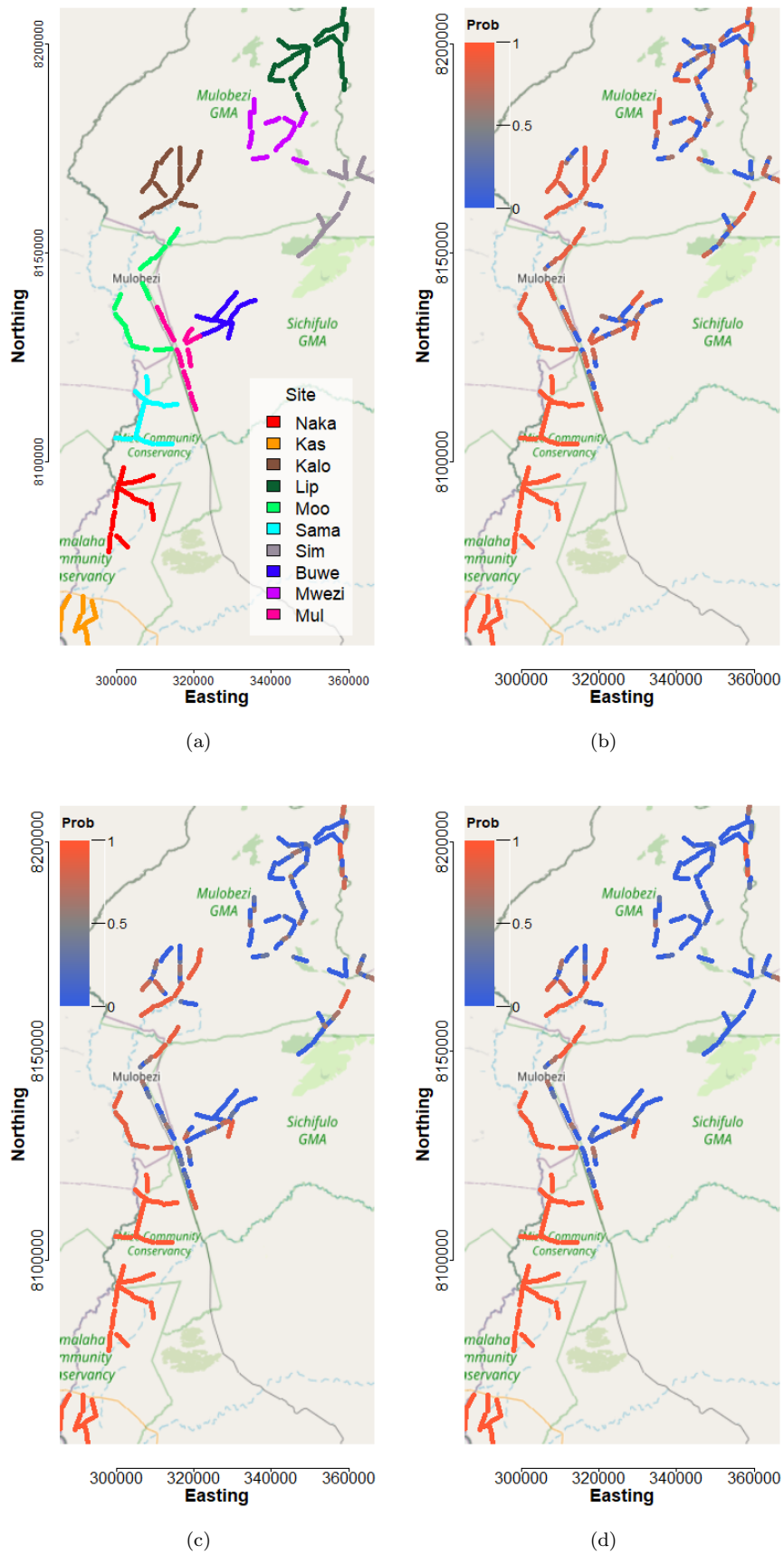


Figure 6. Map of the study area with transect segments coloured according to the (a) site in which they belong, or the posterior probability of segment occupancy from model (b) MP/DND/1, (c) MP/DND/2, (d) MP/DND/3